electronic reprint

Acta Cryst A
FOUNDATIONS
ADVANCES

ISSN: 2053-2733
journals.iucr.org/a

Three-periodic nets, tilings and surfaces. A short review and new results

Olaf Delgado-Friedrichs, Michael O'Keeffe, Davide M. Proserpio and Michael M. J. Treacy

Acta Cryst. (2023). A**79**, 192–202

Acta Cryst A
FOUNDATIONS
ADVANCES

ISSN 2053-2733

Received 5 November 2022
Accepted 17 January 2023

Edited by P. M. Dominiak, University of Warsaw, Poland

Keywords: tilings; nets; 3-periodic nets; 3-periodic tilings; essential rings.

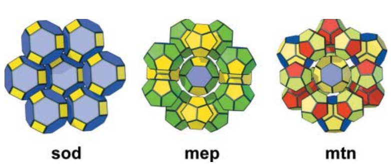

Three-periodic nets, tilings and surfaces. A short review and new results

Olaf Delgado-Friedrichs,[a] Michael O'Keeffe,[b] Davide M. Proserpio[c] and Michael M. J. Treacy[d]*

[a]Department of Materials Physics, Australian National University, Canberra, Australian Capital Territory 2601, Australia, [b]School of Molecular Sciences, Arizona State University, Tempe, Arizona 85287, USA, [c]Dipartimento di Chimica, Università degli Studi di Milano, Milano, 20133, Italy, and [d]Department of Physics, Arizona State University, Tempe, Arizona 85287, USA. *Correspondence e-mail: treacy@asu.edu

A brief introductory review is provided of the theory of tilings of 3-periodic nets and related periodic surfaces. Tilings have a transitivity [p q r s] indicating the vertex, edge, face and tile transitivity. Proper, natural and minimal-transitivity tilings of nets are described. Essential rings are used for finding the minimal-transitivity tiling for a given net. Tiling theory is used to find all edge- and face-transitive tilings ($q = r = 1$) and to find seven, one, one and 12 examples of tilings with transitivity [1 1 1 1], [1 1 1 2], [2 1 1 1] and [2 1 1 2], respectively. These are all minimal-transitivity tilings. This work identifies the 3-periodic surfaces defined by the nets of the tiling and its dual and indicates how 3-periodic nets arise from tilings of those surfaces.

1. Introduction

We are concerned with tilings of 3-periodic nets important in crystal chemistry and the surfaces defined by the nets of dual tilings. Periodic tilings of 3D Euclidean space play an important part in developing the theory of nets (Delgado-Friedrichs *et al.*, 1999). It has been argued that edge-transitive nets – those with only one type of edge (or bond) between vertices (or atoms) – are the most important for the designed synthesis of materials with targeted frameworks (Delgado-Friedrichs *et al.*, 2007).

Identifying tilings associated with periodic nets is particularly useful for developing the systematics of zeolite frameworks (Anurova *et al.*, 2010, and references therein). Periodic foams are particular kinds of tiling. In foams, the tiles (bubbles) are simple polyhedra – all vertices are 3-coordinated. In a foam, also called *simple tiling*, two tiles meet at each face, three at each edge, and four at each vertex. The theory of foams is relevant to many research areas, such as biophysics and materials science (Prud'homme & Kahn, 1996; Cantat *et al.*, 2013).

Three-periodic surfaces are also important in chemistry, biology, materials science and physics (Andersson *et al.*, 1988; Kresge & Roth, 2013; Han & Che, 2018, Al-Ketan & Abu Al-Rub, 2019). Tilings of periodic surfaces also generate 3-periodic nets systematically (Hyde *et al.*, 2006). A significant development was the recognition of new 3-periodic surfaces as defined by a pair of interpenetrating nets (Schoen, 1970). Fischer & Koch (1987, 1989) gave a comprehensive enumeration of such *balance* surfaces (defined by an interpenetrating pair of identical nets). The nets (*labyrinth graphs*) of balance surfaces have self-dual tilings; identifying these is a major concern of this article.

2. Nets, cycles and rings

Nets are considered to be periodic, simple (no loops or multiple edges), connected, finite coordination graphs. In the present context, we consider only graphs that have embeddings in 3D space with linear non-intersecting edges and vertex coordination ≥ 3. Crystallographic and tiling data for all the nets in this paper can be found in the Reticular Chemistry Structure Resource (RCSR), available at http://rcsr.net/ (O'Keeffe *et al.*, 2008). Embeddings of nets with linear, non-intersecting edges are given symbols such as **xyz** or **xyz-w**. We are particularly concerned with the *cycles* of nets – a cycle is a set of edges that begin and end at the same vertex and where each edge occurs only once. To specify *vertex symbols*, a *ring* is defined as a cycle that is not the sum (defined below) of two smaller cycles (O'Keeffe & Hyde, 1997; Blatov *et al.*, 2010). A *strong ring* has been defined as a cycle that is not the sum of any smaller cycles (Goetzke & Klein, 1991).

The sum of two cycles is defined as the set of edges that only occur once (edges common to the two cycles are deleted). More generally, the sum of several cycles is the set of edges that occur an odd number of times. The later discussion shows that a face cycle on a cage is the sum of all the other face cycles. In Fig. 1(*a*), we illustrate some sums in a cube that may be considered a tile of the primitive cubic lattice net (**pcu**). The blue 6-cycle (6 edges) is the sum of two 4-cycles, and hence is not a ring. The red 6-cycle is different: it is not the sum of two 4-cycles but the sum of three 4-cycles, so it is a ring but not a strong ring. The shortest cycle is necessarily a strong ring. Still, it is worth noting that in a periodic structure with infinitely many cycles, the shortest ring can always be expressed as the sum of two larger rings. For example, isolating the cube as a fragment of the net of the **pcu** net, the black 4-cycle in Fig. 1(*a*) is the sum of the red and blue 6-cycles.

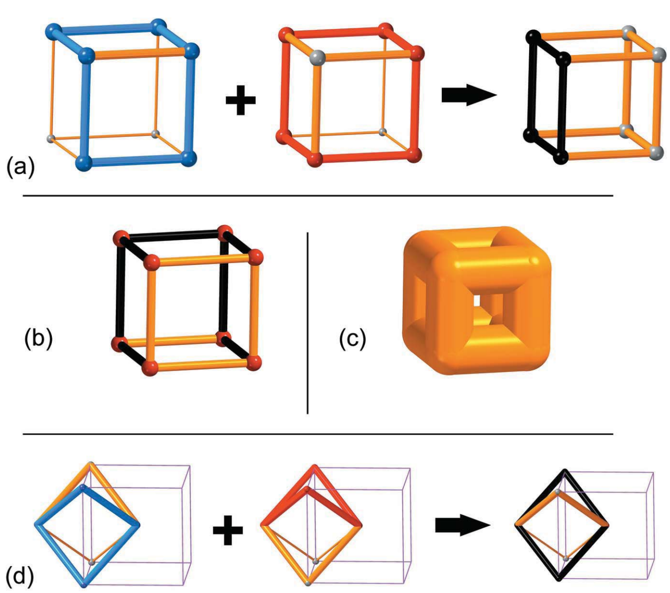

Figure 1
(*a*) Cycles and sums in a cube: the blue cycle is the sum of two 4-cycles (the top and front squares), so is not a ring. The red cycle is the sum of three 4-cycles (the top, front and left squares; or, equivalently, the bottom, back and right squares), so is a ring, but not a strong ring. The sum of the two 6-cyles is the black 4-cycle. (*b*) A spanning tree (black) on the cube graph. (*c*) The cube graph as a surface. (*d*) Cycles in the body-centered cubic net **bcu**: the black 4-cycle is the sum of the red and blue 4-cycles. All 4-cycles in **bcu** are strong rings.

The *genus* of a periodic net is the number of holes in the net in a repeat unit. The genus of a net is defined as the *cyclomatic number* of a repeat unit (*quotient graph*) of the net. The cyclomatic number of a finite graph is $1 + e - v$, where v is the number of vertices and e is the number of edges. It is the minimum number of cycles needed to obtain all the cycles in the graph by cycle sums. A *spanning tree* of a graph is a subgraph without cycles that includes all vertices. The black lines in Fig. 1(*b*) delineate a spanning tree of the cube graph. Five edges need to be added to complete the graph; thus, the cyclomatic number of the cube is $1 + 12 - 8 = 5$. This is the genus of the surface defined by the cube graph – Fig. 1(*c*). To see that the number of independent holes in the surface is five, in the topological sense, imagine starting with a complete cube. Drill a hole from one face to an opposite face – that is one hole. Now drill through a second, orthogonal, pair of opposite faces, intersecting the first hole; that generates an additional two disconnected holes. Finally, drill through the third pair of opposing faces, intersecting the previous two drillings; that, too, creates two more holes for a total of five. In general, the genus of a polyhedron graph is one less than the number of faces.

Taking any five of the six 4-rings of the cube as a basis (there are six combinations possible), all cycles can be obtained as sums of one or more of the chosen basis. The total number of cycles is obtained as follows. Each 4-ring in these sets of five can either be included or omitted, giving $2^5 = 32$ cases. Four cases do not produce a new cycle: there is one case where all rings are omitted; three combinations correspond to pairs of disjoint 4-cycles (opposite faces). This leaves a total of 28 valid cycles.

The cyclomatic number is used in naming cyclic molecules: thus, cubane, the hydrocarbon C_8H_8 with the cube graph, has the formal name pentacyclooctane.

Relevant to later discussion is that the genus of a non-intersecting periodic surface is the same as the genus of its labyrinth graphs. It is the number of holes in the surface in the basic repeat unit of the surface.

3. Tiles in two and three dimensions

In graph theory, a graph is *k-connected* if at least k vertices have to be deleted to decompose the graph into disjoint parts. (To clarify, it is worth reminding the reader that the terms *connected* and *coordinated* describe different graph properties.) A cage with 2-valent (2-coordinated) vertices is 2-connected, as a 2-valent vertex can be separated by deleting its two neighbors. A famous result (Steinitz's theorem) is that a finite planar 3-connected graph is the 1-skeleton of a polyhedron *sensu stricto* (which has an embedding with planar convex faces). An extension to planar 3-connected 2-periodic graphs says that they have embeddings with convex tiles

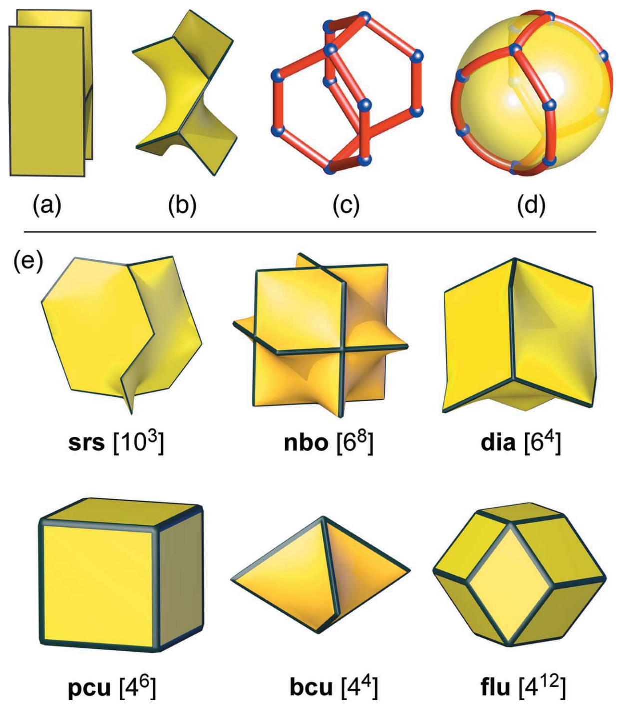

Figure 2
Top row $[6^2.8^2]$ tiles: (*a*) for **cds**, (*b*) for **qtz**. (*c*) The $[6^2.8^2]$ cage, as for **qtz**, drawn with vertices and edges, and (*d*) embedded on the surface of a sphere. The bottom panel (*e*) presents a selection of space-filling tiles of some basic tiling-transitive nets.

(Delgado-Friedrichs, 2005), and 2-valent vertices are generally not allowed in 2D tilings. However, an important development in the theory of 3-periodic tilings was to allow tiles to be *cages*, generalized polyhedra with 2-valent vertices (Delgado-Friedrichs *et al.*, 1999; Delgado-Friedrichs & Huson, 2000).[1] Fig. 2 shows some simple examples of space-filling cages, the tilings of the quartz net (**qtz**) and **cds** nets, and a drawing of the graph of these tiles on a sphere. It should be clear that a face of a tile cannot be catenated to other rings or be knotted. The face symbol of a cage $[p^m.q^n\ldots]$ indicates that there are m faces with p edges, n faces with q edges *etc*. The **qtz** and **cds** tiles are $[6^2.8^2]$.

4. Tilings of nets and periodic surfaces

In a systematic description of the tilings of high-symmetry nets, Delgado-Friedrichs & O'Keeffe (2003) argued that tilings should be composed of strong rings but not all of the strong rings could be included. Thus, in the tiling of the net **bcu**, of the body-centered cubic lattice, only one of the two different strong rings could be used to construct a full-symmetry ($Im\bar{3}m$) tiling. In Fig. 1(*d*), we show a group of edges defining a tile of **bcu**. The faces are non-planar 4-cycles (4A). As shown in the figure, the sum of two of these (red and blue) produces a planar 4-ring (4B black). The tile is $[4A^4]$ and the 4B cycles (strong rings) are not *essential* (not necessary to forming a tiling). One can construct a tiling of **bcu** with tiles $[4B.4A^2]$ if the symmetry is lowered to $C2/m$.

In the Dress–Delgado–Huson description of tilings (Delgado-Friedrichs *et al.*, 1999), the tiling is described by an extended Schläfli symbol, which we call a D-symbol. Each tile is divided into tetrahedral *chambers*, each with four vertices: one at the center of the tile, one at a tile vertex, one at a tile edge center, and one at a tile face center. The *complexity* of the tiling (also known as the *flag transitivity*) is just the chamber transitivity (the number of different types of chambers). Its importance is that, in enumerations of possible tiles of a particular sort, *e.g.*, face-transitive, one proceeds from complexity 1 up to a certain maximum. There is only one 3-periodic tiling of Euclidean space with flag transitivity 1 (*regular* to mathematicians) – the tiling by cubes. Coxeter (1973) refers to this lack of riches, compared with tilings of the plane or the sphere or in higher dimensions, as an 'unfortunate accident'. However, we find richness in tilings of greater complexity, as illustrated herein. It should be stated that the tilings we describe are always face-to-face – that is, all the edges of shared faces are common to both faces.

A tiling has *transitivity* defined by four integers $[p\,q\,r\,s]$ (Delgado-Friedrichs & Huson, 2000). This indicates that there are p kinds (*i.e.* related by symmetry) of vertices, q kinds of edges, r kinds of faces and s kinds of tiles.

A tiling has a *dual tiling* constructed as follows. A new vertex is placed inside every tile of the original, and these are connected to the new vertices in neighboring tiles by an edge that passes through the common face. The faces of the new tiling have separate vertices from the original vertices and have an edge from the original tiling passing through. The symmetry and complexities of a tiling and its dual are the same. The dual of a tiling with transitivity $[p\,q\,r\,s]$ has transitivity $[s\,r\,q\,p]$.

There are two ways to associate a surface with a net. Many nets of interest in crystal chemistry can be considered tilings of a surface (Hyde *et al.*, 2006). In a recent paper (Smolkov *et al.*, 2022), this approach was applied to zeolite nets. Thus, the net **sod** (zeolite framework type **SOD**) was shown to be a $[6^4]$ tiling of the P minimal surface (see Fig. 3). However, a different approach is to consider a net as a surface – think of the edges as thin inflatable tubes. When two nets of dual tilings interpenetrate, the edge tubes can be inflated uniformly until

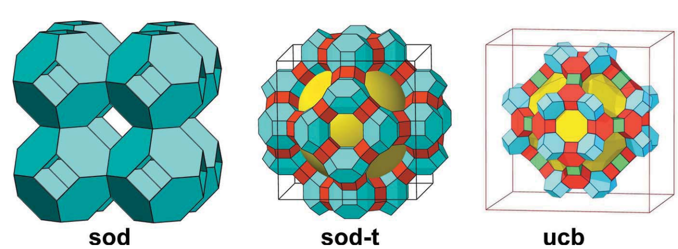

Figure 3
Left: the **sod** framework represented as a $[6^4]$ tiling of the P minimal surface. Center: the **sod-t** tiling of the **sod** surface. Right: another tiling of the **sod** surface.

[1] It might be noted that tilings by 'saddle polyhedra', such as the tiling of the diamond net by adamantane cages, were clearly shown earlier (Pearce, 1980, Fig. 90).

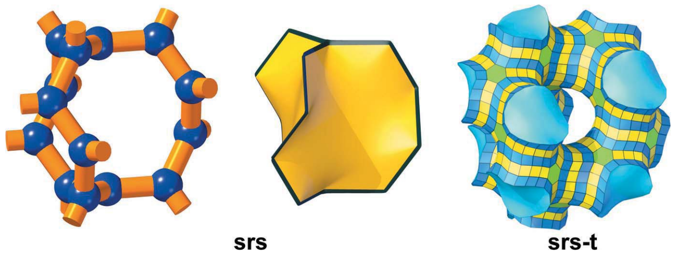

Figure 4
The **srs** and **srs-t** nets. Left: a fragment of the **srs** net. Center: one tile of the **srs** tiling. Right: the corresponding **-t** tiling. Vertex tiles are yellow and green, collar tiles blue.

all tube surfaces are in complete contact, deformed from the initial tubular profile, with no empty spaces between them. If the two nets are the same (related by symmetry), the surface is a *balance surface* (Fischer & Koch, 1987).

A procedure for visualizing a tiling of that resulting surface, the **-t** net, found from chambers of the tiling of the net, has been described (de Campo *et al.*, 2013). Thus, all the chambers' edges and vertices define a periodic graph formed by face-sharing tetrahedra. The **-t** tilings are the dual of the tiling by those tetrahedra, so they are *simple* tilings (tilings by polyhedra in which four meet at a vertex, three at an edge and two at a face). Hence, they are good sources of potential zeolite structures (Delgado-Friedrichs *et al.*, 2020). In Fig. 3, we show the **sod-t** net, a tiling of the **sod** surface. A notable example of a zeolite-like framework which is a tiling of the **sod** surface is afforded by the zeolitic imidazolate frameworks (ZIFs) with the **ucb** net (Yang *et al.*, 2017), also shown in Fig. 3.

Perhaps the most important 3-periodic surface of all is the *gyroid*, or *G* surface, first described by Schoen (1970) and relevant to chemistry, materials science (liquid crystals *etc.*) and biology (*e.g.* bone structure) (Hyde *et al.*, 2008). This is the balance surface separating two **srs** nets. The **srs** net is the only 3-coordinated net that is vertex- and edge-transitive and has the minimal genus (3) for a 3-periodic net. Fig. 4 shows fragments of the **srs** net and the corresponding **-t** tiling. The tiling has two kinds of tile (a tile-transitivity of 2): a *vertex tile* surrounding a vertex of the parent net and a *collar tile* linking two vertex tiles through which an edge of the parent net passes. The collar tile is topologically a prism – in this case, $[4^{20}.20^2]$. Every vertex of the **-t** tiling is on the *G* surface.

The same surface can be associated with more than one net. We illustrate this with the (3,4)-coordinated net **tfc**, with symmetry *Cmmm*. As discussed by de Campo *et al.* (2013), the surface associated with this net is the *P* surface separating two primitive cubic (**pcu**) nets. For **tfc**, we show in Fig. 5 first the tiling with full symmetry; this has just one kind of tile $[8^6]$. The dual tiling is a lower-symmetry tiling of the **pcu** net (symmetry $Pm\bar{3}m$) with the cubes split into three parts, as shown in the figure. The **tfc-t** tiling contains two vertex and two collar tiles, as shown in Fig. 5(*b*). But, as also shown in the figure, three vertex tiles and two collar tiles can be merged into one vertex tile that can, in turn, be linked by six collars to form a slightly distorted version of the *P* surface, although the symmetry of the embedding remains *Cmmm*.

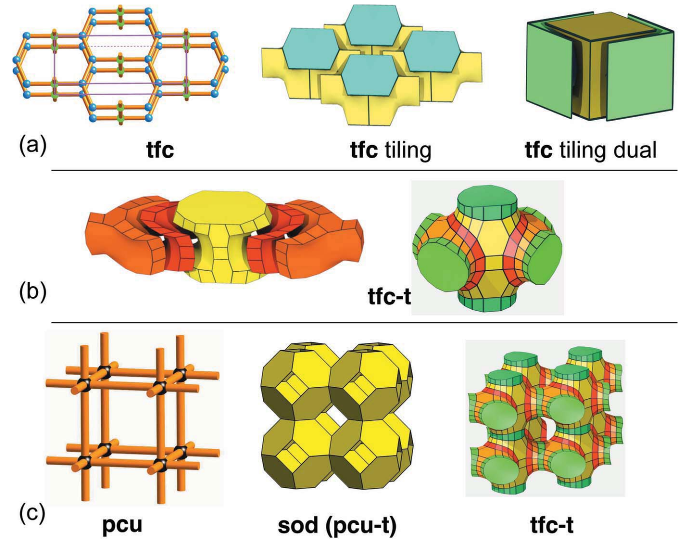

Figure 5
(*a*) The **tfc** net, its tiling and dual tiling. (*b*) Part of the **tfc-t** tiling; vertex tiles are yellow and orange, and collar tiles are red and green. (*c*) The **pcu** net and its **-t** tiling (**sod**) and the **tfc-t** tiling illustrating the *P* surface.

We say that a tiling *carries* a net as the 1-skeleton (vertices and edges), which is unambiguous. Modern tiling theory can systematically enumerate tilings. However, the converse problem of finding a tiling that carries a given net, is not straightforward. If a net admits a tiling, there can be infinitely many. This problem was addressed by Blatov *et al.* (2007), who pointed out that a *proper tiling* should have the symmetry of

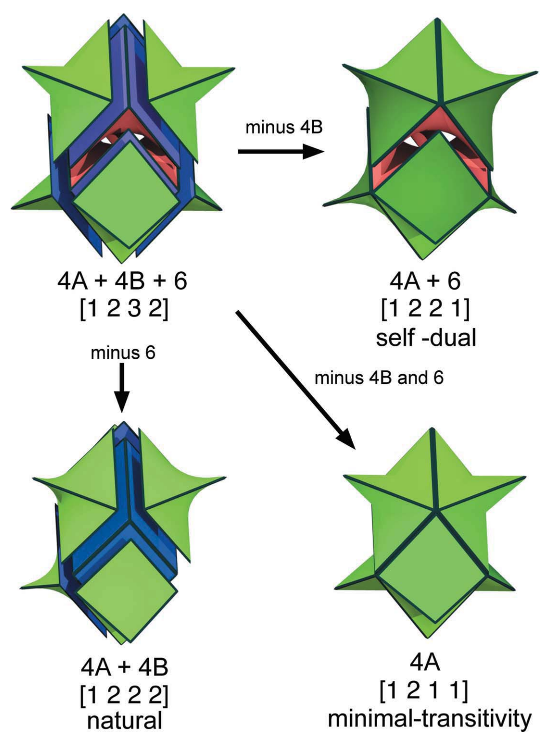

Figure 6
Tilings of the **svn** net. The four-digit numbers are the vertex–edge–face–tile transitivity, [*p q r s*].

Table 1
Edge- and-face-transitive tilings and associated surfaces.

'Trans.' is transitivity and 'coord.' is coordination. A * after a net symbol indicates that the tiling is not a natural tiling, ‡ indicates that the tiling is not proper. For self-dual tilings, the symmetry is first the symmetry of the tiling and then the symmetry of the balance surface. For surfaces, see Fischer & Koch (1989) and Schoen (1970). For genera, see Koch & Fischer (1993).

Trans.	Net	Symmetry	Coord.	Dual	Tiles	Genus	Surface
[1 1 1 1]	**srs**	$I4_132$–$Ia\bar{3}d$	3	Self	$[10^3]$	3	$Y^{**} = G$
[1 1 1 1]	**dia**	$Fd\bar{3}m$–$Pn\bar{3}m$	4	Self	$[6^4]$	3	D
[1 1 1 1]	**pcu**	$Pm\bar{3}m$–$Im\bar{3}m$	6	Self	$[4^6]$	3	P
[1 1 1 1]	**nbo**	$Im\bar{3}m$	4	**bcu**	$[6^8]$	4	I-WP
[1 1 1 1]	**bcu**	$Im\bar{3}m$	8	**nbo**	$[4^4]$	4	I-WP
[1 1 1 1]	**lcy***	$P4_132$–$I4_132$	6	Self	$[5^6]$	9	Y
[1 1 1 1]	**fcu‡**	$Pa\bar{3}$–$Ia\bar{3}$	12	Self	$[3^{12}]$	21	F
[1 1 1 2]	**fcu**	h	12	**flu**	$2[3^4] + [3^8]$	6	F-RD
[2 1 1 1]	**flu**	$Fm\bar{3}m$	4 + 8	**fcu**	$[4^{12}]$	6	F-RD
[2 1 1 2]	**ctn***	$I\bar{4}3d$–$Ia\bar{3}d$	3 + 4	Self	$4[8^3] + 3[8^4]$	11	S
[2 1 1 2]	**pyr**	$Pa\bar{3}$–$Ia\bar{3}$	3 + 6	Self	$2[6^3] + [6^6]$	13	$C(^{\pm}Y)$
[2 1 1 2]	**cys***	$P4_132$–$Ia\bar{3}$	3 + 6	Self	$2[10^3] + [10^6]$	13	$C(Y)$
[2 1 1 2]	**pth***	$P6_222$–$P6_422$ $c' = c/2$	4 + 4	Self	$[4_4] + [4_4]$	7	–
[2 1 1 2]	**ftw**	$Pm\bar{3}m$–$Im\bar{3}m$	4 + 12	Self	$3[4^4] + [4^{12}]$	9	$C(P)$ Neovius
[2 1 1 2]	**mgc***	$Fd\bar{3}m$–$Pn\bar{3}m$	6 + 12	Self	$2[4^6] + [4^{12}]$	19	$C(D)$
[2 1 1 2]	**twf***	$Im\bar{3}m$	4 + 24	**ocu**	$4[4^6] + 3[4^8]$	18	–
[2 1 1 2]	**ocu***	$Im\bar{3}m$	6 + 8	**twf**	$6[4^4] + [4^{24}]$	18	–
[2 1 1 2]	**ibd***	$Ia\bar{3}d$	4 + 6	**iac**	$3[6^4] + 2[6^6]$	29	–
[2 1 1 2]	**iac***	$Ia\bar{3}d$	4 + 6	**ibd**	$3[6^4] + 2[6^6]$	29	–

the net. For many of the nets of greatest interest in crystal chemistry, this tiling is unique but by no means for all. The problem arises because, although the vertices and edges of a net are uniquely defined, there may be many choices of cycles of the net that can form the faces of tiles, and hence alternative proper tilings are possible. It was argued that the faces should be strong rings (Blatov *et al.*, 2007). A *natural* tiling was defined as comprising the smallest tiles (with the fewest vertices) obeying that constraint. For many of the nets encountered in crystal chemistry, this provides a unique tiling, and a procedure was described for treating the exceptions.

To illustrate the possible kinds of proper tiling, we examine the 7-coordinated net **svn** with symmetry $Pa\bar{3}$. The net has two strong 4-rings, 4A and 4B, and a 6-ring that can be used to construct a proper tiling. In Fig. 6, we show that there are four possible proper tilings, including a self-dual (two tiles), a natural (two tiles), and one with minimum transitivity (one tile).

In this article, we introduce a modified version of the proper tiling by establishing the idea of an *essential ring* so that a unique *minimal-transitivity* tiling can be identified. To recall, a *proper* tiling is one that has the same symmetry as the net it carries. A *natural* tiling (*a*) is proper, (*b*) all faces are strong rings, (*c*) has the smallest possible tiles subject to conditions (*a*) and (*b*). A *minimal-transitivity* tiling again (*a*) is proper, (*b*) has faces that are strong rings, but now (*c*) has the minimal number of rings to make a tile. As shown by Blatov *et al.* (2007), for some larger-transitivity nets, there can be more than one possible natural tiling, and additional conditions have to be applied to get a unique tiling. The same problem arises with minimal-transitivity tilings. However, the nets we consider have a unique minimal-transitivity tiling, and we argue below that different tilings of the same net may be appropriate for different purposes.

We extend the concept of an essential ring by stating that if a tile has exactly one face that is different from all the others, that face ring is not essential and can be removed from the tiling by merging tiles. This means that sometimes proper tiles must be merged to create a minimal-transitivity tiling. For example, the net **ctn** has two strong 8-rings, 8A and 8B, and the proper tiling includes the tile [8A.8B^2], as shown in Fig. 7. However, as depicted in the figure, these can be merged into one tile [8B^4]. As another example, the net **lcy** has strong 3- and 5-rings, but the 3-rings are the sum of three 5-rings, and, as shown in Fig. 7, two [3.5^3] tiles can be merged into one [5^6] tile.

A more striking example (Fig. 8) is afforded by the net **cys**, which has strong 4-rings and 10-rings. The proper tiling contains tiles [4^3], [10^3] and [4.10^2]. Using just essential rings, one [4^3] and three [4.10^2] tiles can be merged into one [10^6] tile.

Sometimes, tilings of large-transitivity nets have proper tilings with tiles that have two or more faces that are each different from all the other faces of the tiles, and one or more of these two is essential to avoid infinite tiles, or even to construct a tiling. A complicated example is provided by the tilings of the net of the zeolite **BEA**. A natural tiling has transitivity [9 18 15 8] and 12 of the 18 different rings occur just

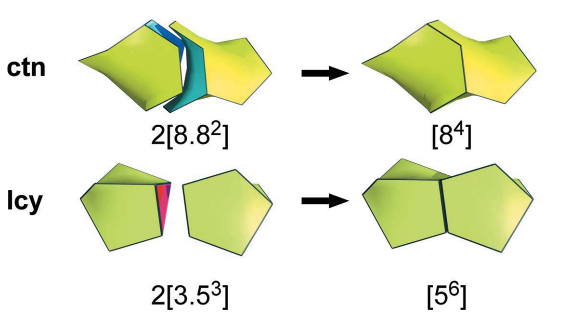

Figure 7
Illustration of the elimination of non-essential strong rings in two minimum-transitivity tilings.

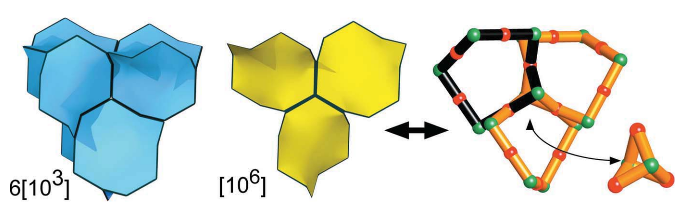

Figure 8
Left: the proper tiling of the net **cys**. Center: the six [10^3] tiles (blue) combine to produce a single [10^6] tile (yellow). Right: the 1-skeleton of the [10^6] tile contains a [4^3] cage of non-essential rings. Red and green vertices are 4- and 6-coordinated in the net.

once in a tile, and one tile has seven faces with all different rings. Clearly, not all of these rings can be eliminated to make a minimal-transitivity tiling. But we emphasize the reason for examining tilings of such high-transitivity nets is to identify the structure-building units, rather than to clarify the taxonomy of symmetrical nets, tilings and surfaces.

5. Minimal-transitivity tilings of vertex-1- and -2-transitive nets and associated surfaces

We have re-examined the earlier list of face-transitive tilings used to generate edge-transitive nets by dualization (Delgado-Friedrichs *et al.*, 2007). This contained all tilings up to a complexity of 32 (recall, ‘complexity’ is the number of distinct tetrahedral chambers into which the tile can be subdivided). We retrieved tilings that were proper and which did not have intersecting or collinear edges. We focused on edge-transitive structures, more specifically, vertex-transitive nets with tiling transitivity [1 1 1 1] and [1 1 1 2], and those with vertex-2-transitive tilings, [2 1 1 1] and [2 1 1 2]. These are, in a sense, the most regular (smallest transitivity). The results are listed in Table 1. Also listed is the associated periodic surface. For structures with transitivity [1 1 1 1], [1 1 1 2] and [2 1 1 1], there are two additional nets to those recognized in the earlier study (Friedrichs *et al.*, 2003). One addition is **lcy**, a minimal-transitivity tiling described above that defines the periodic surface *Y*. The second addition is a non-proper tiling (symmetry $Pa\bar{3}$ instead of $Fm\bar{3}m$) of the net of the face-centered cubic lattice, **fcu**. This tiling is long recognized as one of seven face-transitive tilings by polyhedra (Dress *et al.*, 1993). For the record, the other six are **bcu-x** (tetrahedron*), **reo-d** (octahedron*), **fcu** (tetrahedron + octahedron), **pcu** (cube), **crs-d** (cube*) and **flu** (rhombic dodecahedron). Here, the asterisk indicates that the polyhedron is not in its maximum symmetry. We discuss the surface associated with the $Pa\bar{3}$ tiling of **fcu** below.

Of the ten tilings with transitivity [2 1 1 2], only two were also natural tilings; for the rest, some rings of the natural tiling were not essential to forming a tiling. Particularly pleasing was the recognition of the tiling of the **cys** net (Fig. 8). This net was reported as the labyrinth graph of the C(*Y*) surface (Fischer & Koch, 1987). The **cys** net was not recognized earlier (Delgado-Friedrichs *et al.*, 2007) because it has non-crystallographic symmetries – that is, there are pairs of vertices (green in the figure) that have the same neighbors, so interchanging a pair is an automorphism of the graph but is not a rigid-body symmetry. However, the tiling and associated surface have crystallographic symmetry.

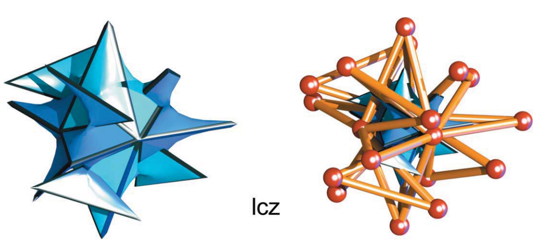

Figure 9
The [5^{12}] tile of the **lcz** net.

It should be recorded that we have omitted one of the [1 1 1 1] tilings from our list. This is a proper tiling, [5^{12}], of the 12-*c* net, **lcz**. This net has strong 3- and 4-rings. These cannot be used to construct a tiling, but a tiling can be built from 5-rings (which are *not* strong rings) in the tiles shown in Fig. 9. The dual structure has coincident edges, and a tiling for the dual cannot be constructed.

The tiling of the net **pth** (Fig. 10) is of interest because the pair of nets, and the associated surface, are the only ones with non-cubic maximum symmetry on our list. The tiles have small dihedral angles, but the **-t** tiling shows a pleasing surface that we have not seen identified before. The **pth-t** tiling has high transitivity [20 32 23 3], so is not, perhaps, a target for synthesis.

The self-dual tiling of **fcu** with symmetry $Pa\bar{3}$ is of interest because the labyrinth graphs (**fcu**) cannot be drawn with straight non-intersecting edges (Bonneau & O’Keeffe, 2015*a*). However, a well defined balance surface separates the two nets; this is illustrated as a **-t** tiling in Fig. 11. The minimal-transitivity tiling of **svn** (Fig. 6) has as a dual the [3^{12}] tiling of **fcu** shown in the figure. The **-t** tiling of this structure is a tiling of the same surface. The tiling is complex (complexity 384) with two vertex and three collar tiles. One vertex tile and associated collar tiles give the same pattern as in the **-t** tiling of the self-dual **pcu**; the second set of vertex tiles are linked in pairs by a collar tile, as shown in the figure, to make a combined tile attached to 12 collar rings. The labyrinth graphs of the two halves are **fcu** and **svn**. We note that the **svn** net is derived from **fcu** by splitting a 12-coordinated vertex into two linked 7-coordinated vertices; accordingly, the genus is unchanged with 1 extra edge and 1 extra vertex.

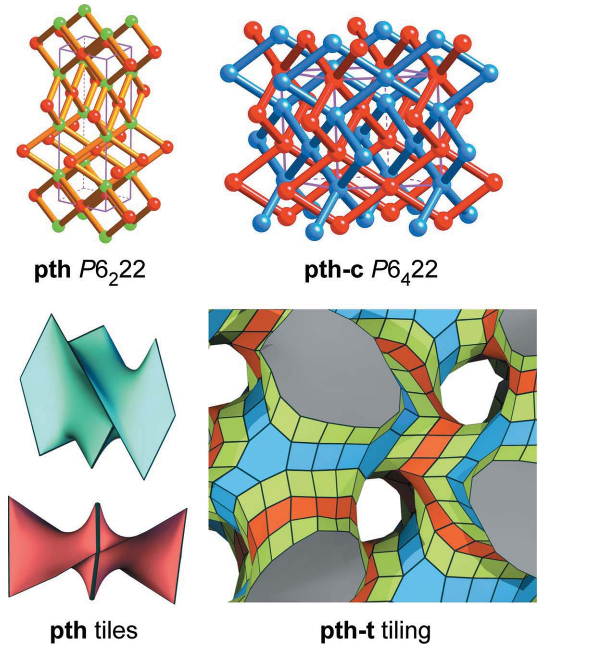

Figure 10
Top: the net **pth** and its symmetric interpenetrating pair. Bottom left: the tiles of the **pth**. Bottom right: the tiling **pth-t** illustrating the balance surface. The vertex tiles are green [$4^{16}.16^2$] and blue [$4^{26}.6^4.16^4$], the collar tile is red [$4^{28}.8^2.16^4$].

Table 2
Additional tilings as discussed in the text.

‡ indicates it is not a proper tiling.

Trans.	Net	Symmetry	Coord.	Dual	Tiles	Genus	Surface
[1 1 2 1]	**sod**	$Im\bar{3}m$	4	**bcu-x**	$[4^6.6^8]$	7	–
[1 2 1 1]	**buc-x**	$Im\bar{3}m$	14	**sod**	$[3^4]$	7	–
[1 1 2 1]	**qtz**	$P6_222$	4	**qzd**	$[6^2.8^2]$	4	Q
[1 2 1 1]	**qzd**	$P6_222$	4	**qtz**	$[7^4]$	4	Q
[1 2 2 1]	**cds**	$P4_2/mcm$–$P4_2/mcm$ $a' = a/\sqrt{2}$	4	Self	$[6^2.8^2]$	3	CLP
[1 2 2 1]	**qtz**‡	$P6_122$	4	Self	$[6^2.8^2] + [6^2.8^2]$	7	Q
[2 2 2 2]	**hms**	$P\bar{6}m2$–$P6_3/mmc$	3 + 5	Self	$[6^3] + [6^5]$	3	H

6. Additional low-transitivity tilings

6.1. Genus-3 and -4 structures cds, hms and qtz

Surfaces of low genus are particularly interesting for the nets carried by tilings of the surface (Hyde *et al.*, 2006). These authors describe the method for systematically enumerating tilings of the genus-3 surfaces P, D and G with tilings of transitivity [1 1 1 1]. It is known (de Campo *et al.*, 2013) that there are just two more genus-3 3-periodic surfaces. They were named CLP and H by Schoen (1970). The nets are **cds** and **hms**. Data for the associated tilings are in Table 2.

The RCSR database lists 41 nets of genus 4. Of these, **bcu** and **nbo** are the only pair with mutually dual tilings. They are listed in Table 1. The only other edge-transitive net of genus 4 is **qtz** (the net of quartz). The **qtz** net has a unique proper tiling with transitivity [1 1 2 1]. The dual tiling carries the net **qzd**. The associated periodic surface has been described by Markande *et al.* (2018), who gave a full description of the non-balance surface defined by the **qtz–qzd** pair. However, two quartz nets of the same handedness related by translation (**qtz-c** in the RCSR) are well known and are frequently found in crystal structures, so it is interesting to ask if a non-intersecting balance surface occurs. To this end, an embedding of the **qtz** net with a doubled c axis and symmetry $P6_122$ was examined. Five distinct tilings were found: three were improper duals of proper tilings, and one was the **qtz–qtz** pair, but there was also a self-dual tiling with transitivity [1 2 2 1]. The surface associated with this latter surface was examined by way of the **-t** tiling, which has symmetry $P6_222$ and transitivity [19 28 22 3]. Two tiles are prismatic collar tiles $[4^{12}.12^2]$ and $[4^{16}.16^2]$. The structure is illustrated in Fig. 12 as a tiling and also as the net of the tiling in an equal-edge, minimal-density embedding drawn as a surface. The **qtz** labyrinth nets can be discerned, and the surface is a balance surface. This is, of course, just a 'balance' embedding of the same surface as that defined by the **qtz–qzd** pair.

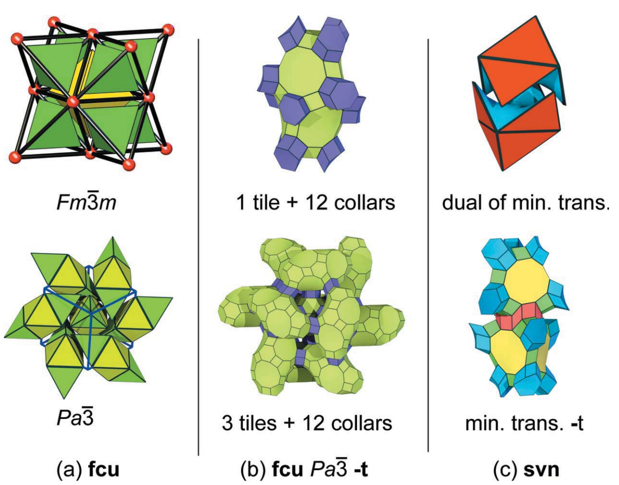

Figure 11
(*a*) Two tilings of **fcu**; yellow and green are octahedra and tetrahedra, respectively. (*b*) Top: a vertex tile (green) and 12 collar tiles (purple). Bottom: 12 more vertex tiles added to the top group. (*c*) Top: the dual of the $[5^{12}]$ tiling of **svn** (Fig. 5). Bottom: the corresponding **-t** tiling showing how two vertex tiles (yellow and green) merge with a red collar net to form one tile linked with 12 blue collar tiles.

6.2. Foams (simple tilings)

The physical chemistry of foams (simple tilings) has been investigated for many years (*e.g.* Weaire & Hutzler, 1999; Cantat *et al.*, 2013). Here, we focus on the geometrical aspects of periodic foams.

Tilings by tetrahedra were systematically enumerated by Delgado-Friedrichs & Huson (2000), who found precisely nine with one kind of tile (isohedral). The dual tilings are simple tilings by polyhedra (foams). Interestingly, seven of the nine are also zeolite framework structures: **CHA**, **FAU**, **KFI**, **LTA**, **RHO**, **SOD** and **RLY** (**sod-a**) (the upper-case, bold, three-letter terminology is that of the Structure Commission of the International Zeolite Association. The three letters match the lower-case nomenclature used in the RCSR database). Of the tetrahedral tilings, just one was also vertex-transitive. The net is the 14-coordinated net of first- and second-nearest neighbors of the body-centered cubic lattice **bcu-x**. The dual tiling has the **sod** net and is the unique vertex-transitive foam with one kind of bubble (isohedral). The associated surface is illustrated in Fig. 3. Data for these two are collected in Table 2.

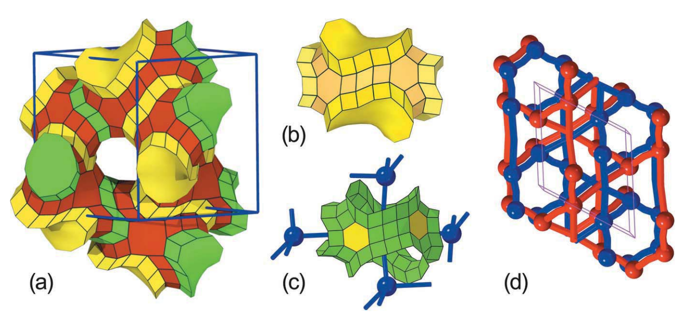

Figure 12
Aspects of the **qtz** balance surface. (*a*) The **-t** tiling of the self-dual **qtz** tiling. Vertex tile red, collar tiles yellow and green. (*b*) One vertex tile and four collar tiles. (*c*) The same with the labyrinth graph (blue). (*d*) The dual **qtz** nets.

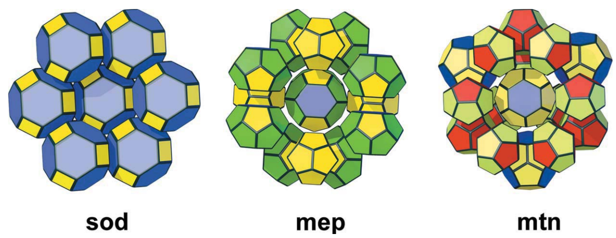

Figure 13
Examples of simple periodic foams.

In isohedral simple tilings, tiles must have at least 14 faces. There are 23, 176 and 710 distinct isohedral tilings, respectively, by tiles with 14, 15 and 16 faces. The **sod** tiling is the unique vertex-transitive isohedral simple tiling. There are 11 vertex-2-transitive isohedral simple tilings (Delgado-Friedrichs *et al.*, 2005).

Tilings by regular polyhedra are called *uniform tilings*. There are 28 of them (Grünbaum, 1994). Of these, four are simple tilings, and three are the tilings of zeolite frameworks (**SOD**, **LTA** and **RHO**).

Simple tilings are relevant to the description of intermetallic structures. Many such structures are space fillings by tetrahedra – sometimes called 'topologically close-packed'. The dual structures are then simple tilings. Many examples are given by Bonneau & O'Keeffe (2015*b*), who provide references to the large body of relevant earlier work. The reason for looking at the dual tiling is that each tile 'belongs' to one kind of atom, and its coordination can be seen readily. Three simple examples are given in Fig. 13. The first, **sod**, is the extended body-centered cubic structure of many metals, notably iron.

The second example, **mep**, is the dual of the Cr_3Si structure. The Cr polyhedron $[5^{12}.6^2]$ shares blue and green faces (it is 'bonded' to other Cr polyhedra) and yellow faces with Si polyhedra $[5^{12}]$. The third example is **mtn**, the dual of the Mg_2Cu structure. The Mg polyhedron $[5^{12}.6^4]$ shares blue faces with other Mg polyhedra and yellow faces with the Cu $[5^{12}]$ polyhedra, and the Cu polyhedra share red faces with other Cu polyhedra. Accordingly, it can be seen that the coordinations are $Mg(Mg_4Cu_{12})$ and $Cu(Mg_6Cu_6)$. We remark that the $MgCu_2$ structure type is chemistry's most populated binary structure type. The **mtn** and **mep** structures occur in many contexts and are known as the type-I and type-II clathrate structures.

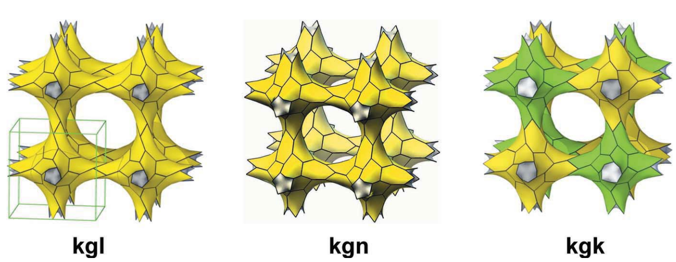

Figure 14
Three different $[7^3]$ tilings of the *P* surface. **kgk** is composed of equal parts of **kgl** and **kgn**, colored yellow and green.

7. Tilings of periodic surfaces

We have already given many examples of tilings of periodic surfaces (Figs. 3, 4, 5, 9, 10, 11, 13) and noted their importance in systematically generating 3-periodic nets (Hyde *et al.*, 2006). Here, we focus on the surface-tiling aspect, but they can be considered infinite polyhedra (Wells, 1977).

We treat first the case of p^3 tilings in which three p-gons meet at each vertex, a subject treated in detail by Hyde & Pedersen (2021). It is worth noting at this juncture that p^n is a vertex symbol, not to be confused with the cage symbol, $[p^n]$, that we used earlier. A cube has vertex symbol 4^3 (three 4-rings at each vertex), but cage symbol $[4^6]$ (a cage bounded by six 4-ring faces). The Euler expression for tiling a 2D surface of genus g with v vertices, e edges, and f faces (tiles) is

$$v - e + f = 2 - 2g = \chi, \quad (1)$$

where χ is the *Euler characteristic*. For a p^3 tiling with n tiles per repeat unit, $v = np/3$ (three p-gons at each vertex, n p-gons per repeat), $e = np/2$ ($e = 3v/2$, as every vertex generates three shared edges) and thus $\chi = n(1 - p/6)$. For $p < 6$ and $\chi = 2$ (tilings of the sphere, genus 0), the possibilities are $p = 3$, $n = 4$ (tetrahedron), $p = 4$, $n = 6$ (cube) and $p = 5$, $n = 12$ (dodecahedron).

For $p = 6$, we get $\chi = 0$, resulting in 6^3 tilings of a surface of genus 1. For a tiling of the plane, this is the familiar honeycomb pattern, net **hcb**. However, for a tiling of the cylinder, also genus 1, there are infinitely many tilings, familiar as the structures of carbon nanotubes. These are all vertex-transitive graphs, even though the nets can lack a translational periodicity (O'Keeffe & Treacy, 2022).

p^3 tilings of surfaces of negative χ ($g > 1$) have been treated in detail by Hyde & Pedersen (2021). Now, for a given p, there may be infinitely many topologically distinct tilings with graphs that are no longer vertex-transitive. We offer a

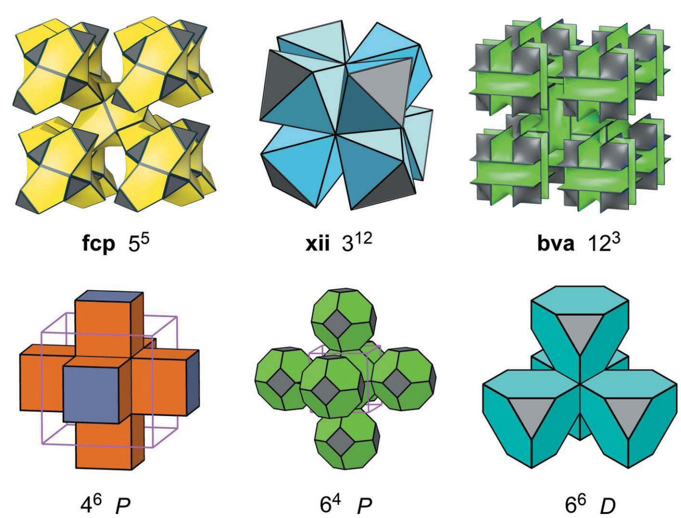

Figure 15
Top row: examples of vertex-transitive tilings of the *I-WP* surface, with vertex symbols. Considered as surface tilings, **fcp** is self-dual, and **xii** and **bva** are mutually dual. Bottom row: regular infinite polyhedra with planar faces.

straightforward example (Hyde & O'Keeffe, 2017) that clarifies that there are infinitely many topologically distinct 7^3 tilings. In Fig. 14, we show two distinct 7^3 tilings (**kgl** and **kgn**) of the *P* surface. Equal-size segments of these two tilings can be linked periodically or randomly into different topologies at will. One example, **kgk**, of an ordered intergrowth, is shown with the different segments colored yellow and green. None of these tilings is vertex-transitive.

Examples of vertex-transitive tilings of the *I-WP* surface are shown in Fig. 15. The 5^5 tiling **fcp** (symmetry $P\bar{4}3n$) is of interest as a vertex-transitive self-dual tiling. It joins 3^3 (tetrahedron, **tet**) and 4^4 (square lattice, **sql**), which are tilings of genus-0 and -1 surfaces, respectively. Note that, as surface tilings (infinite polyhedra), we do not count rings that are not on the surface [*collar rings* (Hyde *et al.*, 2006)], and these three tilings are also face-transitive. Thus, the transitivity as a periodic tiling, [1 3 4 3], becomes [1 3 1] for a surface tiling.

Also shown in Fig. 15 is a 3^{12} tiling, **xii** (symmetry $Im\bar{3}m$). As a 3-periodic tiling, the transitivity is [1 2 3 3], but as a surface tiling (infinite polyhedron), the transitivity is [1 2 1]. Also shown is **bva**, the dual surface tiling 12^3, which also has transitivity [1 2 1].

In tilings of a surface, the chambers become triangles ('flags'). It is straightforward to show (O'Keeffe, 2008) that the only tilings with transitivity [1 1 1] are 4^6, 6^4 and 6^6 tilings of the *P*, *D* and *G* surfaces. Those of *P* and *D* are also flag-transitive. Three of these nine have planar faces and are illustrated in Fig. 15. The 4^6 and 6^4 tilings are dual surface tilings, and the 6^6 surface tilings are self-dual.

8. Methods

We did systematic enumerations of D-symbol tilings. Computing D-symbols is straightforward in principle but suffers from a combinatorial explosion. In practice, the enumeration method must be tailored to the problem. Here, we follow the method for enumerating face-transitive tilings of 3D space described by Dress *et al.* (1993), but we allow tile vertices of coordination 2, whereas they require the coordination to be at least 3. Consequently, a rigorous upper bound on the size of D-symbols that can occur is no longer available to us. Instead, we enumerate up to an arbitrary size that we hope is large enough to cover all relevant solutions.

Dress *et al.* (1993) also refer to the non-trivial problem of determining whether a candidate D-symbol does correspond to a tiling of 3-periodic Euclidean space, which they solve with a combination of automated tests and case-by-case inspection. We use an extended series of computerized tests described by Delgado-Friedrichs (2005) that significantly reduces the number of cases requiring human intervention.

The program *3dt* can illustrate tilings and their duals and export tiling and net data. The symmetry, identity and optimal embeddings of nets are determined by the program *Systre*. Tilings of nets can be determined as coordinates of faces from *Systre* input to the program *ToposPro*.

ToposPro (Blatov *et al.*, 2014) is available at https://topospro.com/. *Systre* (Delgado-Friedrichs & O'Keeffe, 2003) and *3dt* are available at http://gavrog.org/. *3dt* input files for many of the nets in the RCSR and for zeolite nets are available at the RCSR website under the *Systre* link. *ToposPro* can also generate *3dt* input files.

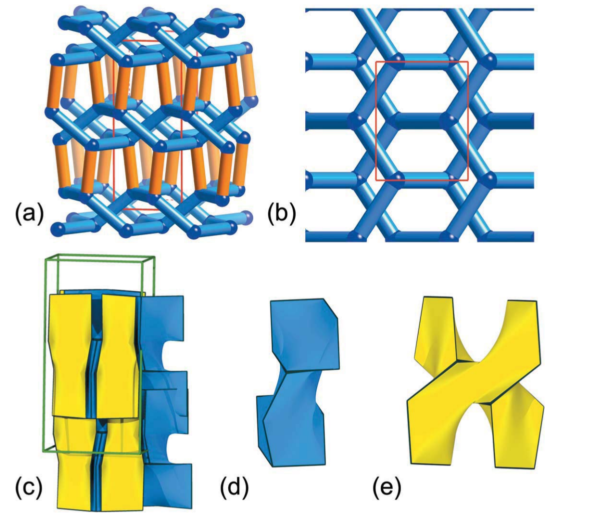

Figure 16
(*a*) The **mok** net, symmetry *Cccm*. (*b*) A layer normal to the crystallographic [010] direction in the **mok** net shows two interpenetrating **hcb** nets. (*c*) Tiling of the **mok** net. (*d*) [$6^2.10^2$] and (*e*) [$8^2.10^2$] tiles. This structure admits a proper tiling, despite the catenation of 6-rings in the **hcb** layers.

9. Concluding remarks

Here we briefly discuss some peripheral, but relevant, topics.

9.1. Which nets admit tilings? Tessellate and decussate nets

It is essential to recognize that only some nets admit tilings. For example, Delgado-Friedrichs & O'Keeffe (2007) found 61 edge-transitive nets in a search of tilings, but the RCSR contains 85. Accordingly, it is natural to ask, 'What factors determine whether an embedding of a net admits a tiling?'. It should be clear that cycles that contain knots or are linked with other cycles cannot serve as the faces of a tile. However, the presence of linked strong rings does not preclude the admission of a tiling.

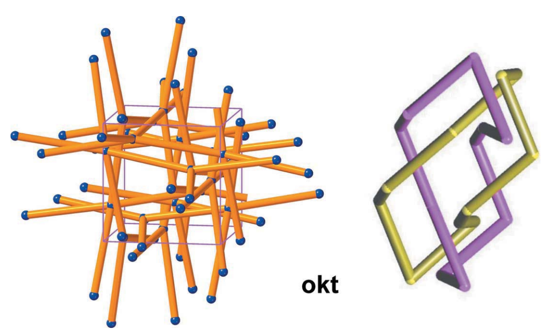

Figure 17
The net **okt.** Left: showing all vertices in a unit cell and their neighbors. Right: two 10-rings catenated in a 4-crossing (Solomon) link.

An example is the net **mok**, introduced originally as an example of a self-entangled net ('link net'; O'Keeffe, 1991). This net, symmetry *Cccm*, has catenated interpenetrating honeycomb (**hcb**) layers normal to **b**, so the **hcb** 6-rings are all catenated. However, there remain non-catenated 6-, 8- and 10-rings which serve as the tile faces, as shown in Fig. 16.

As an example of a net that does not admit a tiling, we adduce **okt**, a 4-coordinated vertex- and edge-transitive net (Fig. 17) not found in the enumeration of tilings. This net contains 10-, 11-, 12-, 14- and 15-rings, but all these are catenated. We propose the terms *tessellate* for embeddings of nets with a tiling, and *decussate* for embeddings of nets for which all embeddings have essential crossings (knots and links) that preclude the construction of a tiling. A given net can have many topologically distinct embeddings. An open problem is whether more than one of these distinct embeddings admits a tiling. We conjecture that a 3-periodic net has, at most, one tessellate ambient isotopy. A related question is whether the only tilings of a net of a certain maximum symmetry are of a lower-symmetry topologically distinct embedding of that net.

9.2. What is the best tiling?

We have reviewed 3-periodic tilings of Euclidean space. There are two kinds: tilings by 3D cages and tilings of 3-periodic surfaces by polygons. Both can be used to generate 3-periodic nets of interest in crystal chemistry systematically. Periodic surfaces can be systematically generated by separating the net of a tiling and the net of the dual tiling. We have shown that when several full-symmetry tilings carry the same net, the minimal-transitivity version is particularly useful.

We show that minimal-transitivity tilings can be found using *essential rings* as the faces. Those with low transitivity are particularly relevant to identifying the simplest ('most regular') periodic nets, tilings and surfaces. However, when considering the gamut of nets in crystal chemistry (*e.g.* Blatov *et al.*, 2014), the generally smaller natural tilings are more appropriate. A striking example is afforded by the tiling of the net **cbo** (the boron net of the zeolite-like structure of CaB_2O_4). The natural tiling (Fig. 18) consists of two tiles, A [3.7^6] and B [$3.6.7^3$], with a transitivity of [1 2 3 2]. The B tile has the unusual property of two rings (3- and 6-rings) occurring only once, so each is the sum of the other tile rings. As shown in the figure, 6-rings can be removed to make a tile B′ [$3^2.7^6$] and produce a tiling of transitivity [1 2 2 2]. A second option is to eliminate the 3-rings having a single tile [$6^2.7^{12}$] and produce a tiling with minimal transitivity [1 2 2 1]. However, a tile of this shape is not likely to be relevant to the systematics of crystal structures, such as zeolites.

As one goes to higher-transitivity nets it is often found that there are multiple proper tilings and choices for either natural tilings or minimal-transitivity tilings. For example, Blatov *et al.* (2007) showed that for the net **eci** there were two candidates with transitivity [1 3 5 2] for a natural tiling. Further examination shows that there are four candidates with transitivity [1 3 3 1] for a minimal-transitivity tiling. However, as we hope we have shown in this article, in the developing systematics and taxonomy of nets and tilings, the relevant feature is not the tilings of nets, but rather the nets of tilings (which are unique), and if, as herein, we seek face-transitive tilings, each will carry a different net. The examples given above are: enumeration of edge-transitive nets, the nets of self-dual and mutually dual tilings, the nets of periodic foams (real and potential zeolite structures) *etc*. On the other hand, in

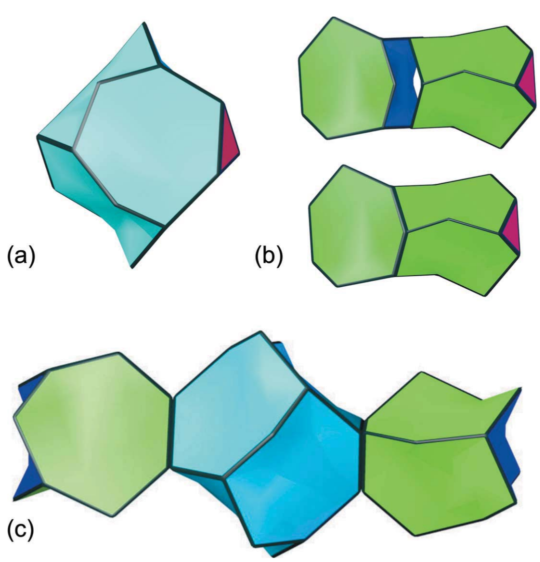

Figure 18
Tilings of the **cbo** net. Three-rings are red, 6-rings dark blue, and 7-rings green and light blue. (*a*) A [$3^2.7^6$] tile. (*b*) Two [$3.6.7^3$] tiles join to form a [$3^2.7^6$] tile. (*c*) The [$6^2.7^{12}$] tile of the minimal-transitivity tiling.

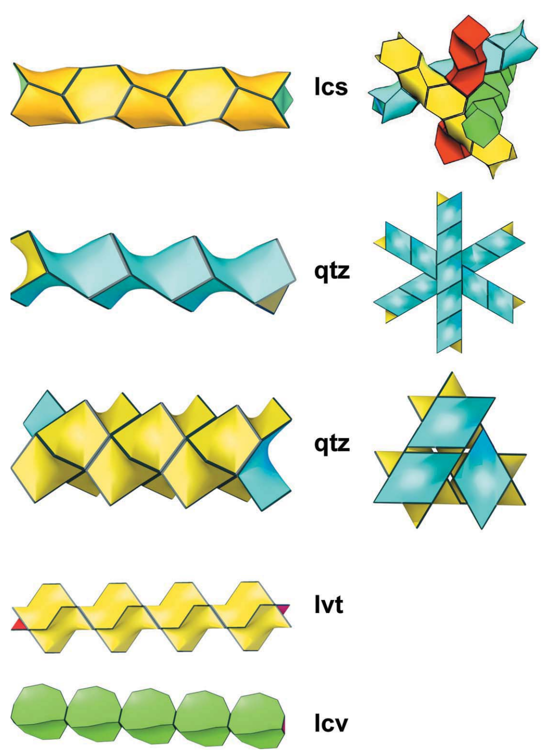

Figure 19
Left: fragments of the infinite tiles described in the text. Right: fragments of the **lcs** and **qtz** tilings.

analyzing the structure-building units of complex frameworks (*cf.* the discussion of the tiling of the net of zeolite **BEA** above) a natural tiling is probably more appropriate.

9.3. Tilings by 1-periodic tiles

Delgado-Friedrichs *et al.* (2002) called attention to a tiling with transitivity [1 1 1 1] of the net **lcs** that had infinite 1-periodic tiles with face symbol [6^∞] packed with axes along the four ⟨111⟩ directions as shown in Fig. 19. One-periodic tiles can be constructed by merging tiles of the sort [$p^2.q^j. \ldots$] with opposite p-ring faces, thereby eliminating these faces. A tiling by such tiles with transitivity [1 1 2 1] can be converted to a [1 1 1 1] tiling by infinite tiles by eliminating the two p-rings.

A search of the RCSR yielded four suitable nets: **lcs** with tiles [$6^2_{\rm A}.6^4_{\rm B}$], **lcv** with tiles [$3^2.10^3$], **lvt** with tiles [$4^2.8^4. \ldots$] and **qtz** with tiles [$6^2.8^2. \ldots$]. The **qtz** admits two tilings by infinite tiles [6^∞] and [8^∞] as shown in the figure. The **lcv** [10^∞] tiles have the same four-way packing as the **lcs** tiles and the **lvt** [8^∞] tiles pack with parallel axes and tetragonal symmetry.

It is noteworthy that the **lcs** tiling by 1-periodic tiles meets the definition of a simple tiling (foam) given above (Section 6). We conjecture that it is then the only such structure with transitivity [1 1 1 1].

Acknowledgements

The authors thank David Palmer for making changes to the *CrystalMaker* software (https://crystalmaker.com/), which was used to generate the framework figures. We thank Professor Vladislav A. Blatov at the Samara Center for Theoretical Materials Science for providing the free *ToposPro* software (https://topospro.com/). *3dt* generated the tiling graphics and, with *Systre*, is freely available at http://gavrog.org/. The free software *POV-Ray* (http://www.povray.org/) generated Figs. 2(*c*) and 2(*d*).

References

Al-Ketan, O. & Abu Al-Rub, R. K. (2019). *Adv. Eng. Mater.* **21**, 1900524.
Andersson, S., Hyde, S. T., Larsson, K. & Lidin, S. (1988). *Chem. Rev.* **88**, 221–242.
Anurova, N. A., Blatov, V. A., Ilyushin, G. D. & Proserpio, D. M. (2010). *J. Phys. Chem. C*, **114**, 10160–10170.
Blatov, V. A., Delgado-Friedrichs, O., O'Keeffe, M. & Proserpio, D. M. (2007). *Acta Cryst.* A**63**, 418–425.
Blatov, V. A., O'Keeffe, M. & Proserpio, D. M. (2010). *CrystEngComm*, **12**, 44–48.
Blatov, V. A., Shevchenko, A. P. & Proserpio, D. M. (2014). *Cryst. Growth Des.* **14**, 3576–3586.
Bonneau, C. & O'Keeffe, M. (2015*a*). *Acta Cryst.* A**71**, 82–91.
Bonneau, C. & O'Keeffe, M. (2015*b*). *Inorg. Chem.* **54**, 808–814.
Campo, L. de, Delgado-Friedrichs, O., Hyde, S. T. & O'Keeffe, M. (2013). *Acta Cryst.* A**69**, 483–489.
Cantat, I., Cohen-Addad, S., Elias, F., Graner, F., Höhler, R., Pitois, O., Rouyer, F. & Saint-Jalmes, A. (2013). *Foams. Structure and Dynamics.* Oxford: Oxford University Press.
Coxeter, H. S. M. (1973). *Regular Polytopes.* New York: Dover Publications.
Delgado-Friedrichs, O. (2005). *Discrete Comput. Geom.* **33**, 67–81.
Delgado Friedrichs, O., Dress, A. W. M., Huson, D. H., Klinowski, J. & Mackay, A. L. (1999). *Nature*, **400**, 644–647.
Delgado-Friedrichs, O., Foster, M. D., O'Keeffe, M., Proserpio, D. M., Treacy, M. M. J. & Yaghi, O. M. (2005). *J. Solid State Chem.* **178**, 2533–2554.
Delgado Friedrichs, O. & Huson, D. (2000). *Discrete Comput. Geom.* **24**, 279–292.
Delgado-Friedrichs, O. & O'Keeffe, M. (2003). *Acta Cryst.* A**59**, 351–360.
Delgado-Friedrichs, O. & O'Keeffe, M. (2007). *Acta Cryst.* A**63**, 344–347.
Delgado-Friedrichs, O., O'Keeffe, M. & Treacy, M. M. J. (2020). *Acta Cryst.* A**76**, 735–738.
Delgado Friedrichs, O., O'Keeffe, M. & Yaghi, O. M. (2003). *Acta Cryst.* A**59**, 22–27.
Delgado-Friedrichs, O., O'Keeffe, M. & Yaghi, O. M. (2007). *Phys. Chem. Chem. Phys.* **9**, 1035–1043.
Delgado Friedrichs, O., Plévert, J. & O'Keeffe, M. (2002). *Acta Cryst.* A**58**, 77–78.
Dress, A. W. M., Huson, D. H. & Molnár, E. (1993). *Acta Cryst.* A**49**, 806–817.
Fischer, W. & Koch, E. (1987). *Z. Kristallogr.-Cryst. Mater.* **179**, 31–52.
Fischer, W. & Koch, E. (1989). *Acta Cryst.* A**45**, 726–732.
Goetzke, K. & Klein, H.-J. (1991). *J. Non-Cryst. Solids*, **127**, 215–220.
Grünbaum, B. (1994). *Geombinatorics*, **4**, 49–56.
Han, L. & Che, S. (2018). *Adv. Mater.* **30**, 1705708.
Hyde, S. T. & Cramer Pedersen, M. (2021). *Proc. R. Soc. A*, **477**, 20200372.
Hyde, S. T., Delgado Friedrichs, O., Ramsden, S. J. & Robins, V. (2006). *Solid State Sci.* **8**, 740–752.
Hyde, S. T. & O'Keeffe, M. (2017). *Struct. Chem.* **28**, 113–121.
Hyde, S. T., O'Keeffe, M. & Proserpio, D. M. (2008). *Angew. Chem. Int. Ed.* **47**, 7996–8000.
Koch, E. & Fischer, W. (1993). *Acta Cryst.* A**49**, 209–210.
Kresge, C. T. & Roth, W. J. (2013). *Chem. Soc. Rev.* **42**, 3663–3670.
Markande, S. G., Saba, M., Schroeder-Turk, G. & Matsumoto, E. A. (2018). arXiv:1805.07034.
O'Keeffe, M. (1991). *Z. Kristallogr.-Cryst. Mater.* **196**, 21–38.
O'Keeffe, M. (2008). *Acta Cryst.* A**64**, 425–429.
O'Keeffe, M. & Hyde, S. T. (1997). *Zeolites*, **19**, 370–374.
O'Keeffe, M., Peskov, M. A., Ramsden, S. J. & Yaghi, O. M. (2008). *Acc. Chem. Res.* **41**, 1782–1789.
O'Keeffe, M. & Treacy, M. M. J. (2022). *Symmetry*, **14**, 822–841.
Pearce, P. (1980). *Structure in Nature is a Strategy for Design.* Cambridge: MIT Press.
Prud'homme, R. K. & Kahn, S. A. (1996). *Foams: Theory, Measurements, Applications*. New York: Marcel Dekker Inc.
Schoen, A. H. (1970). NASA Technical Note No. D-5541.
Smolkov, M. I., Blatova, O. A., Krutov, A. F. & Blatov, V. A. (2022). *Acta Cryst.* A**78**, 327–336.
Weaire, D. & Hutzler, S. (1999). *The Physics of Foams*. Oxford: Clarendon.
Wells, A. F. (1977). *Three Dimensional Nets and Polyhedra.* New York: Wiley.
Yang, J., Zhang, Y.-B., Liu, Q., Trickett, C. A., Gutiérrez-Puebla, E., Monge, M. Á., Cong, H., Aldossary, S., Deng, H. & Yaghi, O. M. (2017). *J. Am. Chem. Soc.* **139**, 6448–6455.